



Microstructural analysis of nanostructured ZnO thin films

M.A. Urbina-Yarupetan¹ and J.C. Gonzalez*^{2,3}

¹Universidad Nacional Mayor de San Marcos, Facultad de Ciencias Físicas. Ciudad Universitaria, Lima - Perú

²Universidad de Ingeniería y Tecnología (UTEC), Laboratorio de Física de Materiales e Ingeniería de Superficies. Barranco, Perú

³Instituto de Ciencia de Materiales de Sevilla – CSIC, Grupo de Investigación de Superficies, Intercaras y Láminas Delgadas. Calle Américo Vespucio 49, Isla de la Cartuja. Sevilla 41092 – España

Recibido 02 mayo 2020 – Aceptado 15 junio 2020

Abstract

We present the experimental results obtained from microstructural analysis of ZnO thin films with 20, 50, and 100 nm in thickness, grown onto the commercial glass substrate by reactive sputtering. We analyze the quantitative information on the size of the crystalline domains, the texture direction of the nanocolumns, their densities, thicknesses, surface and interface roughness obtained through characterization techniques such as scanning electron microscope (SEM), X-ray reflectivity (XRR) and X-ray diffraction (DRX).

Keywords: reactive magnetron sputtering, ZnO thin film, SEM, XRR, XRD.

Análisis microestructural de películas delgadas nanoestructuradas de ZnO

Resumen

Presentamos los resultados experimentales obtenidos del análisis microestructural de películas delgadas de ZnO con 20, 50 y 100 nm de espesor, crecidas sobre el sustrato de vidrio comercial por pulverización catódica reactiva. Analizamos la información cuantitativa sobre tamaño de los dominios cristalinos, dirección de textura de las nanocolumnas, sus densidades, espesores, rugosidad superficial e interfacial obtenida a través de técnicas de caracterización como la microscopía electrónica de barrido (MEB), la reflectividad de rayos X (XRR) y la difracción de rayos X (DRX).

Palabras clave: pulverización catódica reactiva, capas delgadas de ZnO, MEB, XRR, DRX.

Introduction

Thin-film technology is an area in the field of materials science and engineering where extensive growth has been observed [Gon20] given its important industrial applications in different fields of technology, such as microelectronics and integrated circuits [Hua16], high-density magnetic and magneto-optical storage [Per15], surface improvement and protection [Sul10], optics [Ism13], sensor and detector technology [Alh10]. However, thin-films engineering is complicated by the fact that growth physics is not yet well understood in some cases, or research on these growth processes is still ongoing [Alv14].

Therefore, a clear understanding of the growth procedure will allow determining the growth morphology of nanostructured ZnO on difficult substrates, such as commercial glass. Then, to contribute to the knowledge of the thin film growth technology, a microstructural study was carried out on nanostructured ZnO thin films deposited onto commercial glass by magnetron sputtering with variable thickness (20 nm, 50 nm, and 100 nm) by using characterization techniques such as scanning electron microscope (SEM), X-ray diffraction (XRD) and X-ray reflectometry (XRR), in order to correlate properties such as texture, thickness, superficial and interfacial roughness, and density.

*juanc.gonzalez@icmse.csic.es

Experimental

ZnO thin films were grown onto commercial glass (high-quality soda-lime-based silicate glass) by reactive magnetron sputtering technique under conditions that closely resemble those used in industry, which was 300 W of discharge power applied to the Zn target of 3-inch in diameter, in order to produce a power density of 6.50 W/cm^2 . The partial pressure values of argon and oxygen gases were established as the minimum pressures that ensure that the deposit is made in the reactive mode; a ratio of 1:0.80 between argon and oxygen gases was used, so

the optimal value for Zn was $8 \times 10^{-4} \text{ mbar}$. The residual vacuum pressure was $5 \times 10^{-6} \text{ mbar}$ and the ZnO films were deposited with thicknesses of 20, 50 and 100 nm. Also, a ZnO film with 800 nm in nominal thickness was grown in order to obtain only SEM cross-section microimages, because films with a thickness below 100 nm do not have a good resolution to perform SEM cross-section microimages, so this film gives us a clear idea of nanocolumns in their first growth stages until to 100 nm. The area of the samples was approximately $5.0 \times 5.0 \text{ cm}$. Table 1 summarizes the experimental conditions of thin film deposition.

Material	Target	Total Pressure (mbar)	O ₂ Pressure (mbar)	Power (W)	Power Density (W/cm ²)
ZnO	Zinc	1×10^{-3}	8×10^{-4}	300	6.5

Table 1: The experimental conditions of sputtering.

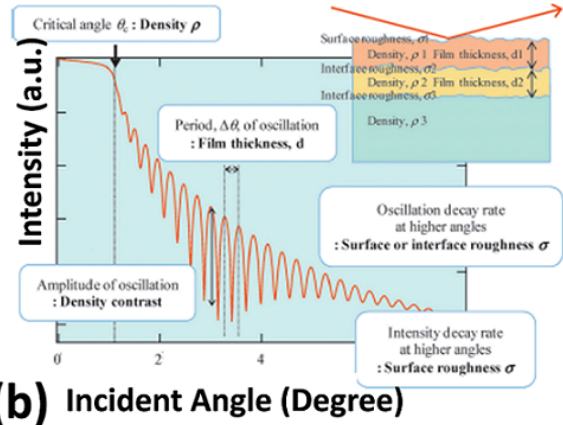
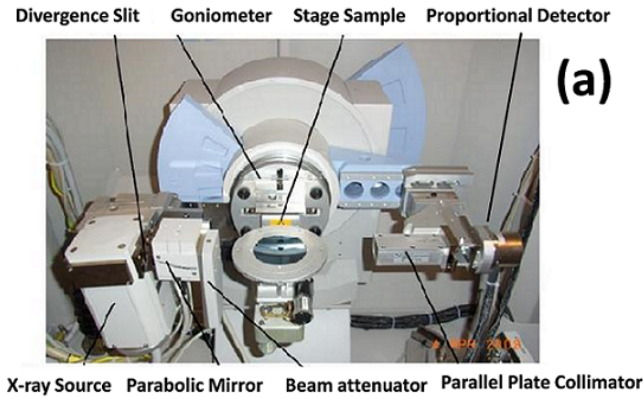


Figure 1: a) Experimental XRR setup, and b) Information provided by X-ray reflectivity profile (Adapted from reference [Yas10]).

Microstructural analysis of ZnO thin films was performed through a scanning electron microscope (SEM), Hitachi S4800 SEM-FEG model, and two X-ray diffractometers. The first diffractometer is a PANalytical X'Pert Pro MPD diffractometer with Cu- $K\alpha$ radiation, in Bragg-Brentano geometry, provided with an X'Celerator detector and graphite monochromator. The range measured was $2\theta_i = 10^\circ$ to $2\theta_f = 80^\circ$ and step value $\Delta 2\theta = 0,016^\circ$. The second one is also a PANalytical X'Pert Pro MRD diffractometer working in reflection mode (scan $\omega - 2\theta$), using Cu- $K\alpha$ radiation and W/Si crystal as an X-ray parabolic mirror, with an X'Celerator detector (Figure 1a). Scan axis was 2θ and scan mode was continuous with a scan range of 0.0° to 5.0° and a step size of 0.005° . The X'Pert reflectivity program [Pan07] was used to fit the reflectivity raw data. Fig-

ure 1b summarizes all the information that we can obtain from X-ray reflectivity profile [Yas10] such as density of the film, thickness, surface and interface roughness. X-ray reflectivity profile for the ZnO thin films was modeled by means of three uniform and homogeneous films or layers with well-defined borders (Figure 2).

Layer 3	ZnO
Layer 2	ZnO
Layer 1	ZnO
Glass	

Figure 2: Layer model used to fit reflectivity spectra.

Results and Discussion

SEM cross-section microimage illustrates the nanocolumnar microstructure and packaging morphology, as we see in Figure 3. A first observation is about the nanocolumn widths, which are in the order of 50 nm, and they grow directly onto the glass surface. The shadows at bottom and at upper of the microimage is directly related to electrostatic charge on the surface of the sample. All the sample is not conductor (ZnO is semiconductor, and glass is dielectric) so the electrons reaching the surface are repelled by the electrostatic negative charge on the surface; as a consequence of the sample charged, it does not allow to obtain a good microimage by the secondary electrons, who are responsible for the formation of the SEM microimage.

X-ray diffraction spectra in Bragg-Brentano geometry are shown in Figure 4. All three samples have well-defined diffraction profiles and wide peaks, the latter correlates well with ZnO columns sizes in the order of nanoscale (Figure 3). Also, a preferential growth in (002) direction or film texture in (002) direction was observed. This texture signal observed is due to the high intensity of (002) reflection compared to other profiles present such as (102) , (211) , and (220) . The preferential growth is on account of the intrinsic nature of sputtering deposition conditions [Alv14]. The (211) profile is the maximum reflection in the powder diffraction file of the ZnO compound, but it is not greater in intensity than the preferential growth (002) direction of ZnO films. The result is that ZnO unit cells grown in the nanocolumns

with its c -axis perpendicular to the surface of the glass substrate. On the other hand, the crystalline domain size has been obtained by using the Scherrer equation through the analysis of (002) reflection. The results show that the crystalline domain size is approximately 50 nm, so the crystalline domains of the three thin layers of ZnO are in the order of nanometers (Table 2), correlating with the SEM microimage in Figure 3.

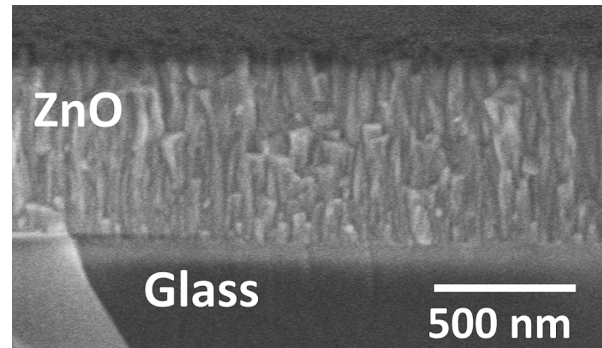


Figure 3: SEM cross-section microimage of ZnO film.

Film nominal thickness (nm)	Crystal domain size (nm)
20	4.0
50	4.7
100	4.6

Table 2: Crystal domains sizes.

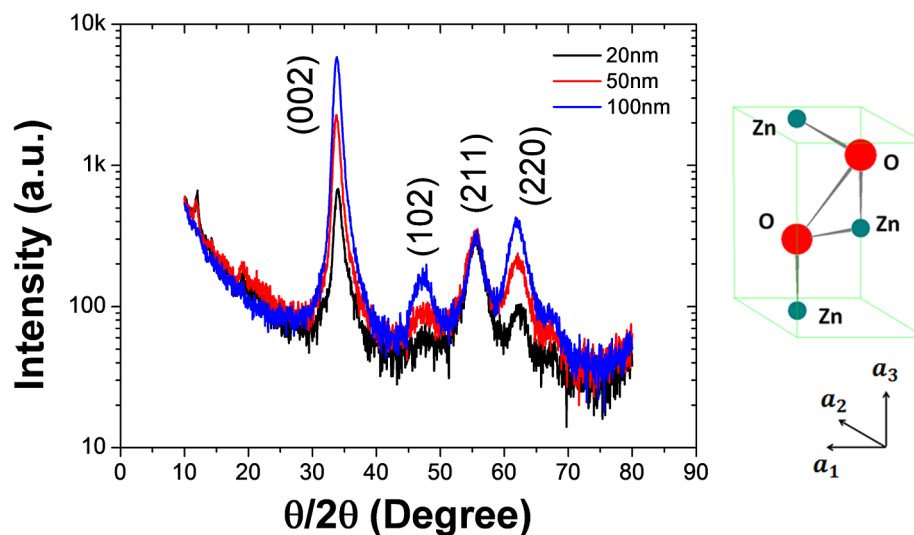


Figure 4: X-ray diffraction diffractogram in Bragg-Brentano geometry and ZnO hexagonal unit cell.

On the other hand, the hexagonal unit cell of ZnO was drawn by using the *PowderCell* program [Kra98]. The ZnO unit cell contains two Zn^{2+} atoms and two O^{2-} atoms, the (002) plane contains one Zn atom and O atom (Figure 4). In addition, it has a space group number equal to 186 and space group equal to $P6_3mc$. The cell parameters are $a = 0.3289$ nm and $c = 0.5307$ nm [Kis89], and the cosine directors are: $\alpha = 90^\circ$, $\beta = 90^\circ$, and $\gamma = 90^\circ$.

The X-ray reflectivity curves are presented in Figure 5. There is a rapid attenuation of the interference oscillations in the film with 100 nm with respect to 20 nm. This fact might be related to the morphology of the imperfect packing of the grown nanocolumns observed in the micrograph of Figure 3. Moreover, another possible cause of rapid attenuation is directly related to the thin film density, that is, a higher density of ZnO particles have accelerated and reached the glass substrate as we increase the thickness of the thin film. In addition, when a lower attenuation of the interference oscillations is observed in an X-ray reflectivity spectrum, it is an indication that we have a more homogeneous thin film and have a better packaging morphology.

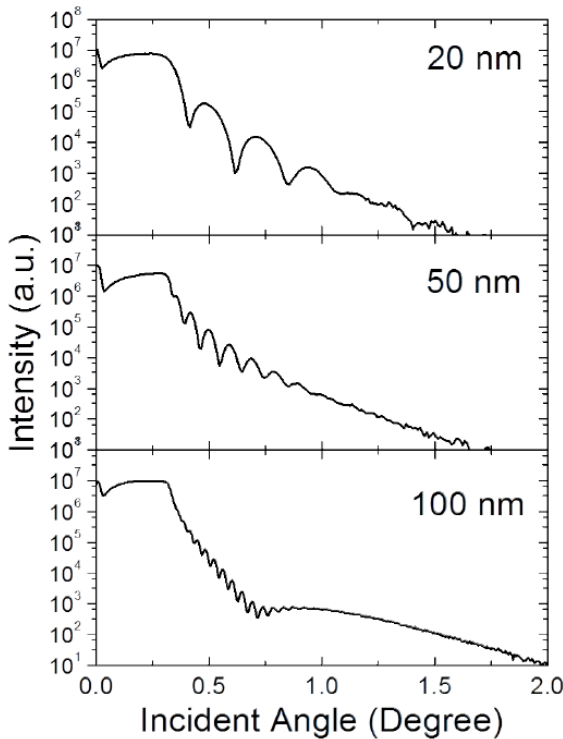


Figure 5: X-ray reflectivity spectra of ZnO thin films.

In Figure 5, each curve was modeled by using three uniform layers with well-defined borders (Figure 2). The thin-film model by three uniform layers was decided by try and error method; we fitted the curves with other

numbers of uniform layers, starting with one until five layers. The lowest value of the figure of merit, as is the mean square error (χ^2), was obtained when the films were modeled with three layers. The fit allowed us to deduce the variations in density with depth, in each of the three layers by using the Reflectivity software [Pan07] from *Panalytical*. The simulations were performed fitting four parameters simultaneously, which were: 1) thickness, 2) density, 3) surface roughness, and 4) interface roughness. Figure 6 presents the fitted X-ray reflectivity spectra (blue curve is the experimental data while the red curve is the fit) according to the criteria considered for the modeling of thin-film described in the previous paragraph. As we can see in Figure 6, the interference oscillations were lost below approximately $2\theta_f = 1.2^\circ$, reason for which we did not perform any fit below this angle. Similarity, the initial incident angle was not necessarily $2\theta_i = 0^\circ$, as in case of samples with a nominal thickness equal to 20 nm ($2\theta_i = 0.20^\circ$), and 50 nm ($2\theta_i = 0.15^\circ$), but it was $2\theta_i = 0^\circ$ in the only case of film with nominal thickness of 100nm. The value of the figures of merit (χ^2) for the three thin films of 20, 50, and 100 nm was 0.9977, 0.9965, and 0.9947 respectively.

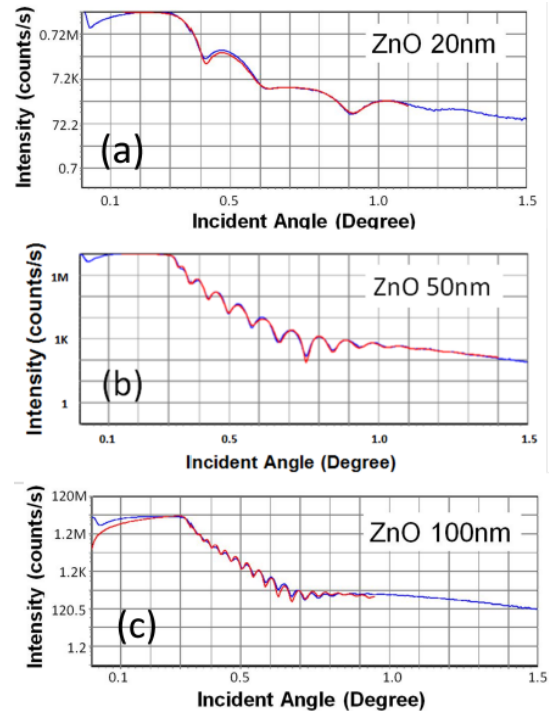


Figure 6: X-ray reflectivity spectra, where blue curve is the experimental data and red curve is the fit.

Table 3 presents the experimental values of the four parameters (thickness, density, surface and interface roughness) obtained after adjusting the specular reflectivity spectra of the three oxide samples. The first col-

umn of Table 3 shows the nominal values of the thicknesses of the three oxides; the second column shows the real thickness for each of the 20, 50 and 100 nm films, the result shown is the sum of the partial thicknesses of the three modeled layers, where we find a variation of 14.25%, 8.28%, and 3.59% in thickness, respectively, with respect to their nominal value. The third column shows the value of the average density of the three modeled layers, we can find a variation of 8.50%, 4.95%, and 4.95% respectively, if we compare these experimental values with the density bulk value of ZnO equal to 5.06 g/cm³, these density results are directly correlated with

Nominal Thickness (nm)	Real Thickness (nm)	Density (g/cm ³)	Surface Roughness (nm)	Interface Roughness (nm)
20	17.15	5.53	1.36	1.85
50	46.85	5.51	1.62	1.50
100	96.41	5.51	2.07	1.12

Table 3: Experimental values obtained from the fit of X-ray reflectivity spectra.

The fourth column of Table 3 indicates the surface roughness of the three thin films around 2 nm approximately, therefore the roughnesses found are in the order of 3 to 4 times the c parameter of ZnO unit cell, these roughness values are so low and they are characteristic of films grown by the sputtering technique. Finally, the fifth column expresses the values of interface roughness, that is, roughness between the oxide layer and the glass substrate, which is in the order of 2 to 3 times the c parameter of ZnO unit cell, that is, less at 2.0 nm. Again, this roughness value gives information that, due to the roughness at the interface, it is possible to obtain ZnO nanocolumns growth in a packed and dense way on the surface of the glass substrate, correlating this information with the microimage in Figure 3.

Conclusions

SEM cross-section microimage illustrates the nanocolumnar microstructure and packaging morphology, and nanocolumns widths were in the order of 50 nm, and they grew directly onto the glass surface. X-ray diffraction showed well-defined diffraction profiles, and good crystallinity, as well as a textured growth of the films in the direction (002), also allowing to obtain the crys-

taline domain size, through of the Scherrer equation, which is in the order of 5.0 nm. The analysis of the X-ray reflectivity curves through the modeling of a ZnO film as three uniform layers with well-defined borders, allowed us to determine the true value of the thickness, the average density increased to 5.0% with respect to the theoretical density, then nanocolumns were packing, as well as the surface and interface roughness values. These last two values were in the 2.0 nm range, i.e., a very low roughness.

Acknowledgments

Authors deeply thanks to three agencies: British Council (UK), CONCYTEC FONDECYT (Perú) and Consejo Superior de Investigaciones Científicas (Spain) whom funded the research projects: Nanostructured magnetic thin films of functional oxide for developing of electronic devices based on spintronic; and Crecimiento de nanoestructuras columnares mediante la técnica de magnetron sputtering con aplicaciones tecnológicas; and Planar photonic structures for development of optofluidics sensors and harnessing of solar energy, respectively.

References

[Alh10] Al-Hardan, N., Abdullah, M., Abdul Aziz, A., Ahmad, H., Low, L. (2010) ZnO thin films for

VOC sensing applications. *Vacuum* **85**, 101. <https://doi.org/10.1016/j.vacuum.2010.04.009>

[Alv14] Alvarez, R., Lopez-Santos, C., Parra-Barranco,

- J., Rico, V., Barranco, A., Cotrino, J., Gonzalez-Elipe, A., Palmero, A. (2014) Nanocolumnar growth of thin films deposited at oblique angles: Beyond the tangent rule. *J. Vac. Sci. Technol. B* **32**, 041802. <https://doi.org/10.1116/1.4882877>
- [Gon20] Gonzalez, J.C., Llosa, M., Peña, A. (2020) The hidden potentiality of coatings *Rev. Inv. Fis.* **23**, 2, 7 - 9. https://fisica.unmsm.edu.pe/rif/previo_files/2020-2/05gonzalez.pdf
- [Hua16] Huang, R., Sun, K., Kiang, K., Morgan, K., de Groot, C. (2016) Forming-free resistive switching of tunable ZnO films grown by atomic layer deposition. *Microelectronic Engineering* **161**, 7 - 12. <https://doi.org/10.1016/j.mee.2016.03.038>
- [Ism13] Ismail, A., Abdullah, M. (2013) The structural and optical properties of ZnO thin films prepared at different RF sputtering power. *Journal of King Saud University - Science* **25**, 209. <https://doi.org/10.1016/j.jksus.2012.12.004>
- [Kis89] Kisi, E., Elcombe, M. (1989) U parameters for the wurtzite structure of ZnS and ZnO using powder neutron diffraction. *Acta Crystallogr. C* **45**, 1867. <https://doi.org/10.1107/S0108270189004269>
- [Kra98] Kraus, W., Nolze, G. (1998) PowderCell 2.0 program. Free distribution software. Web http://www.ccp14.ac.uk/ccp/web-mirrors/powdcell/a_v/v_1/powder/e_cell.html
- [Pan07] X'Pert Reflectivity software version 1.2. (2007) PANalytical B.V. The Netherlands. Web <http://laboratorytalk.com/article/269215/software-makes-x-ray-reflectom>
- [Per15] Perriere, J., Hebert, C., Nistor, M., Millon, E., Ganem, J., Jedrecy, N. (2015) $Zn_{1-x}Fe_xO$ films: from transparent Fe-diluted ZnO wurtzite to magnetic Zn-diluted Fe_3O_4 spinel. *J. Mater. Chem. C* **3**, 11239. <https://doi.org/10.1039/C5TC02090E>
- [Sul10] Ugur, S., Sarsik, M., Hakan-Aktas, A., Cigdem-Ucar, M., Erden, E. (2010) Modifying of Cotton Fabric Surface with Nano-ZnO Multilayer Films by Layer-by-Layer Deposition Method. *Nanoscale Res Lett* **5**, 1204. <https://doi.org/10.1007/s11671-010-9627-9>
- [Yas10] Yasaka, M. (2010) X-ray reflectivity measurement, part V in X-ray thin-film measurement techniques. *The Rigaku Journal* **26** (2), 1.